

Urban Modification of the Surface Energy Balance in the West African Sahel: Ouagadougou, Burkina Faso

B. OFFERLE

Urban Climate Group, Physical Geography, Göteborg University, Göteborg, Sweden, and Atmospheric Science Program, Department of Geography, Indiana University, Bloomington, Indiana

P. JONSSON AND I. ELIASSON

Urban Climate Group, Physical Geography, Göteborg University, Göteborg, Sweden

C. S. B. GRIMMOND

Atmospheric Science Program, Department of Geography, Indiana University, Bloomington, Indiana

(Manuscript received 16 August 2004, in final form 14 March 2005)

ABSTRACT

Surface-atmosphere energy exchanges in Ouagadougou, Burkina Faso, located in the West African Sahel, were investigated during February 2003. Basic knowledge of the impact of land cover changes on local climate is needed to understand and forecast the impacts of rapid urbanization predicted for the region. Previously collected data showed a large dry season urban heat island (UHI), which dramatically decreased with the onset of the rainy season and corresponding changes to the natural land cover thermal and radiative properties. Observations of local-scale energy balance fluxes were made over a residential district, and building surface temperatures were measured in three separate locations. Net all-wave radiation showed an increase with urbanization owing to the higher albedo, lower heat capacity, and thermal conductivity of the bare dry soil compared to the urbanized surface. The combination of material and geometry resulted in a decrease in albedo toward the urban center. Despite the higher albedo, surface temperatures of bare undisturbed soil could exceed surface temperatures in the residential area and urban center by 15°–20°C due to differences in thermal characteristics. Turbulent heat exchange measured over a residential area was dominated by sensible heat flux. Latent heat fluxes were greater than expected from the amount of vegetation but in accordance with water use in the area. An urban land surface scheme reproduced fluxes in agreement with measurements. The results point toward an intensification of the dry season urban heat island in Ouagadougou, given increased urbanization.

1. Introduction

Although there has been an expansion of urban field campaigns in recent years, relatively little research has been conducted in the dry Tropics. This is a concern because, although urbanization is increasing worldwide, these increases are much more marked in less developed countries. Within sub-Saharan Africa, the average annual urban growth rate (4.8%, 1980–93) was higher than in any other region of the world (Binns et al.

2003). These rapid rates of urban growth have led to progressive deterioration of urban and periurban environments (Binns et al. 2003). However, these rapid changes generally occur in the absence of any planning with respect to indoor or outdoor thermal comfort (Ahmed 2003). Along with increased population, population density, and land cover conversion comes, by necessity, increased reliance on nonlocal building materials, all of which play a role in contributing to local urban climate change. In rural Burkina Faso people rely predominantly on local building materials (clay brick, thatch) that have more similar characteristics (albedo and thermal properties) to the natural surroundings than do “modern” materials such as reinforced concrete and corrugated metal roofing. To some extent,

Corresponding author address: Brian Offerle, Urban Climate Group, Physical Geography, Earth Sciences Centre, Göteborg University, Box 460, Göteborg, 405-30 Sweden.
E-mail: oaf@gvc.gu.se

this is also true toward the outskirts of larger towns, marking a transition between wholly traditional construction and more convenient modern materials that do not require as much routine maintenance, although internal building climate may be degraded.

This transition will have an impact on the surface energy balance through the alteration of surface properties affecting net all-wave radiation and heat storage, and consequently impact local climate. It has been noted that land surface and atmospheric alteration by urbanization leads to the development of distinct urban climates (Landsberg 1981; Oke 1987; Helbig et al. 1999). Ultimately these urban climate effects are due to differences in the budgets of heat, mass, and momentum between the city and its preexisting landscape (Oke 1987).

The urban heat island (UHI), perhaps the most distinctive urban climate feature, is associated with the differences between the urban surface and its surroundings. For tropical semiarid cities, the UHI shows strong seasonal differences between wet and dry seasons (Jauregui et al. 1992). Typically the UHI reaches its maximum intensity during the dry season although both wet and dry season heat islands may exist. The seasonal changes are attributed to the seasonal variation in the thermal characteristics of the rural surface (Jauregui et al. 1992). During the dry season the rural soil surface is typically unvegetated and very dry, allowing rapid heating of the surface but with little heat penetrating to any significant depth due to the low thermal conductivity. The surface also cools rapidly at night. As the dry soil has a lower heat capacity, the amount of heat that can be stored and released over a day is small. The drier soil may also have a higher albedo, lowering the absorbed solar energy.

In contrast, the urban surface shows little seasonal change with respect to thermal characteristics. The larger amount of exposed surface, due to the vertical structure of buildings and increased thermal mass, allows for large amounts of heat to be stored and released over the diurnal cycle. Thus land use, and associated land cover change, brought out by the growth of urban areas through in-migration and population growth, may cause local climate change. Although land use change need not lead to observable changes in local climate if radiative and thermal characteristics are only slightly modified. In cities where UHI effects are not observed, the explanation is that the surface characteristics of rural and urban areas are similar (Nasrallah et al. 1990).

The objective of this study is to examine how the city of Ouagadougou, located in the hot, semiarid environment of the West African Sahel, differs from the surroundings in terms of surface-atmosphere energy ex-

change. The study is limited to the dry season period when urban-rural temperature differences are most pronounced. This research initially focuses on measurements of surface temperature at the building scale. By scaling and using the observed temperatures for modeling, heat storage is estimated at the local scale. These observations and model estimates are then linked to energy balance fluxes at the local scale.

2. Geography, climate, and land cover characteristics

Ouagadougou, Burkina Faso (population ~1 million: 12°22'N, 1°31'W; 300 m above sea level) is located in the Sahel, a roughly defined geographical region encompassing the semiarid region of West Africa south of the Sahara. The designation Sahel typically includes the countries of Senegal, Gambia, Guinea-Bissau, Cape Verde, Mauritania, Mali, Burkina Faso, Niger, Chad, and the northern parts of Nigeria (Fig. 1). Within this zone mean annual rainfall ranges from 350 to 800 mm (Ben Mohamed et al. 2002) and is highly variable (Nicholson and Grist 2001; Ben Mohamed et al. 2002).

In Ouagadougou, mean annual rainfall is 782 mm with a range of 355 to 1185 mm over the years 1902–2002 (Vose et al. 1998). During the dry season, and particularly from January to March, the climate is very dry (averaging 0 days of rainfall, Fig. 2) and dusty resulting from the Harmattan wind blowing from the Sahara. Mean air temperature during February is 27.6°C; it ranged from 25.5° to 30.6°C over the period 1949–90 (Fig. 2).

The central business district (CBD, Fig. 3a) has few tall buildings with most from 2 to 4 stories (<15 m) in height. Buildings are concrete and rebar-framed and concrete block construction. Roofs are flat, either corrugated steel or concrete. Streets in the downtown are mostly asphalt, with a few covered with cobble or un-surfaced compacted soil and 20–25 m wide (building to building). In contrast, most of the surrounding residential areas (Fig. 3b) contain a mix of traditional and modern construction. Residences are predominantly single story, and although constructed with cement they may have a higher percentage of aggregate from local material. Roofs are almost exclusively corrugated steel. Nearly all secondary streets are unpaved and have low canyon aspect (height to width, H:W) ratios. In these residential neighborhoods and periurban areas (Fig. 3c), the representative building unit is a compound composed of several small structures, some very densely packed, with open living space and trees for shading within the periphery. The compound is often enclosed by a wall joining the structures (Fig. 4). In newer, wealthier residential areas and along the main

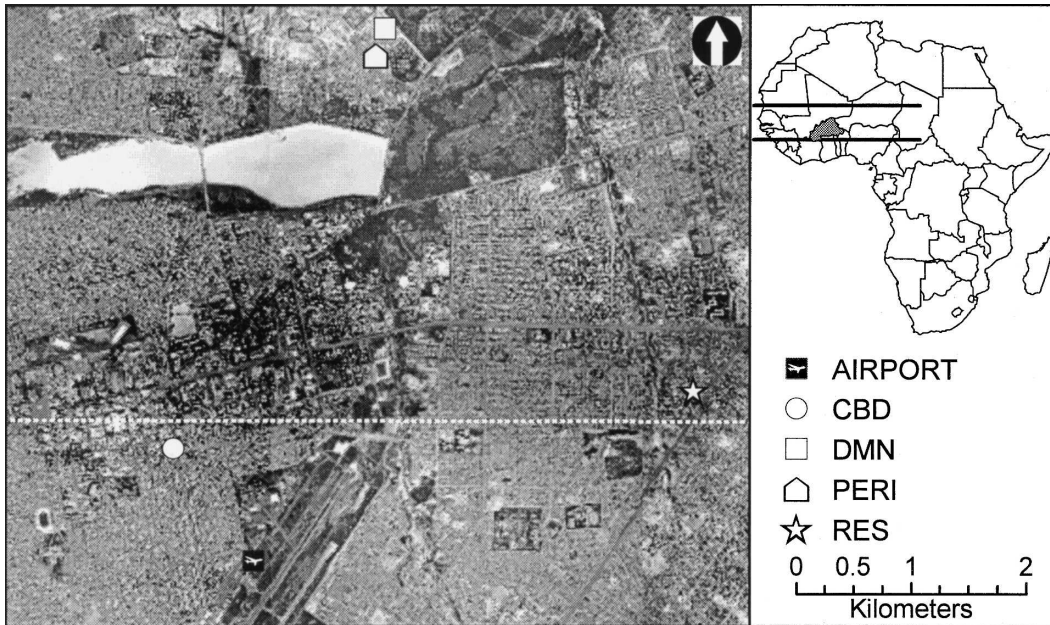


FIG. 1. Mosaicked aerial photographs of a portion of Ouagadougou showing measurement sites and transect (dashed line). The transect extends beyond image edges. Burkina Faso is darkened on the inset map of Africa and the lines show the approximate geographic extent of the Sahel (10° – 18° N).

arterial and ring roads, larger multistoried residential dwellings are common.

In Burkina Faso the annual population growth rate was more than 5% for the years 1975–90 and is projected to remain above 2% (UNPOP 2002). The current rate of population growth in Ouagadougou is estimated at 6.8% (Gerstl 2001). This population growth, coupled with in-migration to the urban area, has fueled marked changes in land cover in recent years. Satellite imagery from 1980 to 1995 showed that changes occurred both within the periphery and more substantially along the main roads around the city (Van

Deursen et al. 1999). The corresponding changes in land cover from urban to residential to periurban are very evident in aerial photographs (Fig. 3). The transition from periurban to residential is marked by a reduction in vegetation and scattered buildings, which over time become increasingly dense, and trees, because of their shade value, are encouraged.

3. Methods

a. Land cover and surface characteristics

Determination of land cover characteristics was based on analysis of aerial photographs and Advanced Spaceborne Thermal Emission and Reflection Radiometer (ASTER) satellite imagery (January and November 2001). The presence of vegetation is expected to vary substantially seasonally in accordance with rainfall patterns except in areas of the city where vegetation is primarily irrigated, such as near the reservoir or within or around compounds in a few neighborhoods. The normalized difference vegetation index (NDVI) can range from above 0.4 to less than 0.1 toward the end of dry season (Eklundh and Olsson 2003). The percentage of vegetation cover within Ouagadougou was determined from the ASTER (January 2001 image) derived NDVI (Chrysoulakis 2003). Tree cover, which should not vary seasonally, was visually identified from aerial photographs (October 1998) and used to specify a relation between NDVI and active vegetation. Building

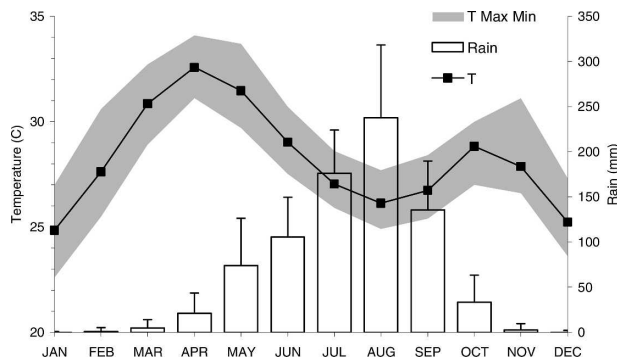


FIG. 2. Long-term monthly mean air temperature and total rainfall. The range for air temperature is the maximum and minimum monthly mean. Error bars for rainfall are +1 std dev. Data from GHCN version 2 (Vose et al. 1998).



FIG. 3. Aerial photographs showing measurement sites: (a) central business district; (b) residential showing the ring road; (c) periurban area. Note the differences in building densities between the residential and periurban development. Scale is the same for all photos. Photographs taken shortly after the onset of the dry season (Oct 1998).

coverage was determined by digitizing building outlines on aerial photographs that were georeferenced to the ASTER imagery. Owing to the small size of the buildings in the residential and periurban areas, often less than 25 m^2 , the values for building coverage are less certain in these areas. The January ASTER image was used to estimate the broadband albedo using the approach of Liang (2000). Other building characteristics were determined from measurements of the individual structures, such as, wall thickness and building height.

b. Measurements

The instrumentation setup was designed to investigate two separate scales of the urban energy balance: an

individual building and its immediate environs (hereafter, building scale) and local scale, which has a length scale of a few hundred to a few thousand meters and so encompasses the effects of multiple buildings and their surroundings. The building-scale measurements included building facet (roof, walls) surface temperature (T_s) and internal wall, room air temperature (T_{ai}) and ground temperature (T_0). External facet temperatures were measured with infrared thermocouples (IRTC, Omega OS36SM or Raytek Thermalert CI) and internal temperatures were measured with thermocouples (TC). The infrared temperatures were not corrected for differences in emissivity. Although the sheet metal used for roofing could have a lower emissivity than the in-

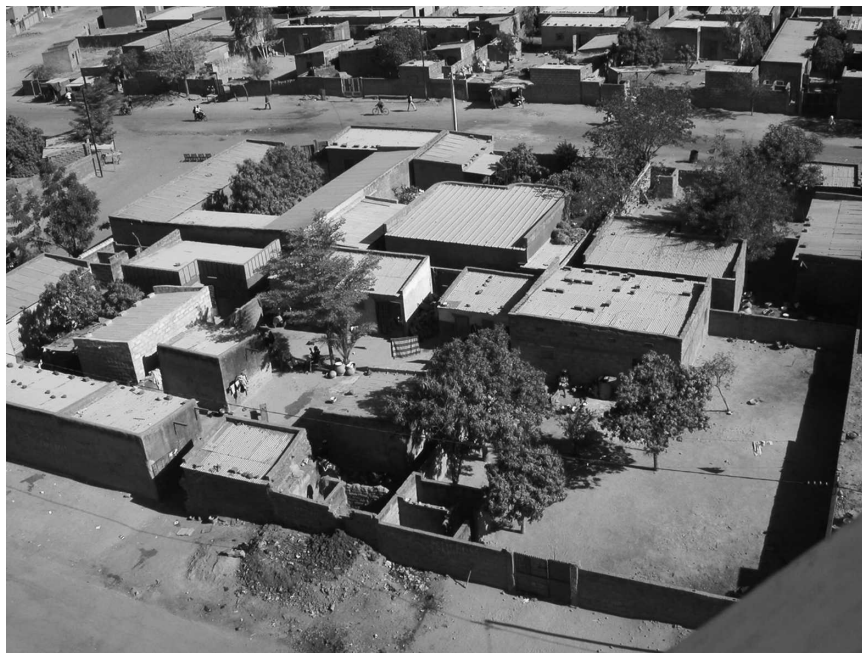


FIG. 4. Compound houses in Ouagadougou.



FIG. 5. Downtown structure used for building-scale heat storage measurements.

strument calibration, owing to the accumulation of dust and oxidation of the metal, the emissivity of the surface is increased. The temperature measurements were made for two building types: 1) a typical residential dwelling and 2) a concrete construction located downtown. For type 1, measurements were made in two separate locations, one in a periurban area (PERI) near the office of the Direction de la Météorologie Nationale (DMN), and a second in residential neighborhood within the city's ring road (RES). Both buildings were similar to those shown in Fig. 4. Building type 2 was a rooftop structure on a three-storey building (CBD, Fig. 5) but included the roof temperature from an adjacent building similar to the majority of downtown roofs. All the structures were of similar size with a plan area of around 25 m^2 and a height of approximately 3 m. The two residential structures were generally not occupied during the daytime. The structure at CBD was unoccupied except for brief periods to retrieve data.

Local-scale measurements of turbulent sensible (Q_H) and latent heat fluxes (Q_E) were made using eddy covariance techniques at a height of 18 m, from a 32-m tower adjacent to the lot containing RES (Fig. 3b). An RM Young model 81000 sonic anemometer was used to measure three-dimensional wind velocity and a Campbell Scientific krypton hygrometer was used to measure water vapor fluctuations. Data were logged at 10 Hz and postprocessed to calculate 30-min fluxes (Offerle et al. 2005). To correct for oxygen absorption in the water vapor spectrum, the coefficients given for k_o in van Dijk et al. (2003) for the hygrometer were applied. Incoming solar radiation ($K\downarrow$, Li-Cor 200SA), net all-wave radiation (Q^* , Radiation and Energy Balance Systems

$Q^*7.1$), air temperature (T_a), and relative humidity (RH) (Rotronic 100MPH), and wind speed (WS) were measured at CBD and RES, and at the DMN climate station. Additional data were collected from the meteorological station at the airport, approximately 2 km southwest of the CBD site. For the seasonal urban – rural temperature differences, air temperature measurements (TinyTag, Gemini Dataloggers) were made from February 2002 to January 2003 in the CBD, at the airport, and at an agricultural station approximately 10 km to the north of the city (Kamboince, not shown). The radiation instruments were compared at DMN at the end of the measurement campaign and data corrected based on ordinary least squares estimates for the linear relation. Locations for the measurement sites within Ouagadougou are shown in Figs. 1 and 3. Table 1 lists the measurements at each site. During the measurement period there was a single rain event with scattered precipitation on 13 February 2003 (DOY 44) lasting from approximately 1600 to 2100 local time. Mean air temperature measured over the campaign at CBD was 30°C , a little more than 2°C warmer than the February climatological average. Clear skies predominated until DOY 44 and were partly to mostly clear thereafter. However, incoming solar radiation, even on clear days, varied presumably due to the variability of dust and water vapor in the atmosphere. Over the measurement period, absolute humidity ranged from 3 to 23 g m^{-3} .

c. Modeling

Neglecting latent heat storage due to moisture changes, the amount of heat stored in a building is proportional to the mass (ρV) of its component elements

TABLE 1. Observed variables by location. See text for variable abbreviations. The approximate observations height (z) is also given. Surface cover fraction is given for vegetation (V), buildings (B), paved roads (R), and bare soil (S). Scale is either building (B) or local (L).

Site	Surface cover	Scale	z (m)	Dates (DOY)	Variables observed
CBD	V < 0.1	B	10	37–47	T_s (N, E, W, S walls), T_{ai}
	B = 0.4			37–50	Q^* , $K\downarrow$, T_a , RH, WS, T_s (roof), T_0 (road)
	R = 0.2				
	S = 0.3				
RES	V = 0.1	L	18	39–51	Q^* , $K\downarrow$, Q_H , Q_E , WS, T_0 (x3)
	B = 0.3			42–50	
	R < 0.1	B	—	47–50	T_s (N, E, W, S walls), T_{ai}
	S = 0.6				
PERI	V < 0.1	B	—	35–41	T_s (N, E, W, S walls, roof), T_{ai}
	B = 0.2				
	S = 0.8				
RUR (DMN)	S = 1	B	2	50–52	Q^* , $K\downarrow$, T_a , RH, wind, T_0
			2	36–57	Q^* , $K\downarrow$, $L\downarrow$, T_a , RH, wind

(e.g., roof, walls, floors, internal mass, internal air), their temperature (T), and heat capacity (C). The total heat storage is an additive combination of the element heat storage. The temperatures of the elements can be determined from the one-dimension heat conduction equation (Fourier's law) if the thermal properties of the materials and both surface boundary conditions are known. In this case, only external temperatures are measured on all five building surfaces (walls and roof) and one or two internal surface temperatures are measured to determine how well internal surface temperature is coupled to internal room air temperature. The local-scale heat storage flux (ΔQ_S , $W m^{-2}$) can be determined by scaling the building, road and soil, and air

heat storage fluxes based on their fractional volumes within the urban canopy layer:

$$\Delta Q_S = \sum_i \frac{\Delta T_i}{\Delta t} (\rho C)_i \Delta x_i \lambda_{pi}, \quad (1)$$

where the term $\Delta x_i \lambda_{pi}$ represents the average depth of element i over the area in question (Offerle 2003). Table 2 lists the estimated thermal properties of materials for buildings and areas. The effects of radiation geometry are implicitly included in the model if the measured surface temperatures are representative of the surface as a whole. For CBD this was not the case owing to the location of the structure. However, the

TABLE 2. Structural and thermal characteristics used for heat storage estimation and TEB. Albedo and roughness length (z_0) apply only to TEB model runs. Model parameters for PERI differ only from RES where noted (*).

Site	Storage element	Material	Δx (m)	k ($W K^{-1} m^{-2}$)	ρC ($J K^{-1} m^{-3}$)	Plan area fraction	Albedo
CBD $z_H = 10$ $z_0 = 1.0$	Wall	Concrete and plaster	0.20	1.0	1.53	1.0 (ext) 2.0 (int)	0.20
	Roof	Reinforced concrete	0.15	1.0	1.53	0.4	0.25
	Ground	Road (asphalt) soil	0.05	1.25	1.2	0.6	0.08
			0.25	0.8	1.2		
			1.25	0.8	1.5		
RES and PERI $z_H = 3$ $z_0 = 0.6$	Wall	Concrete blocks	0.20	0.8	1.53	0.4 (ext) 0.1 (int)	0.25
	Roof	Metal sheet	0.003	5.0	2.07	0.3, 0.2*	0.25
	Ground	Road and soil	0.05	0.6	1.2	0.7, 0.8*	0.25, 0.28*
			0.25	0.6	1.2		
			1.25	0.8	1.5		
RUR	Ground	Soil	0.05	0.4	1.2	1.0	0.28
			0.25	0.6	1.2		
			1.25	0.8	1.5		

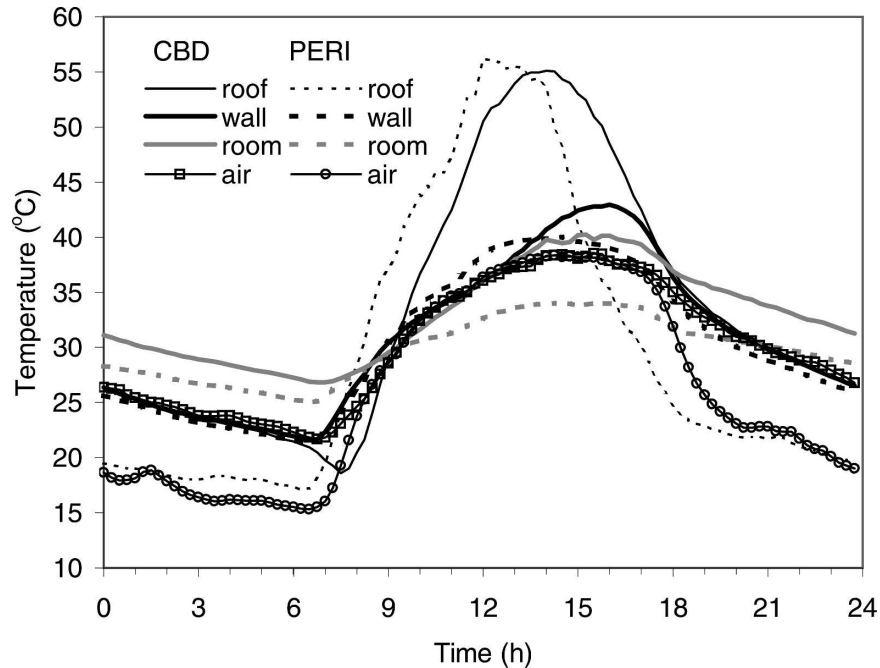


FIG. 6. Building-scale ensemble mean diurnal temperature observations (wall is the mean of four walls, room is inside room air temperature) over 2003/37–42.

increased radiation loading on this structure is at least partially offset by increased turbulent exchange. Where representative road and soil surface temperatures were not measured (e.g., PERI), the surface temperature and, consequently, heat storage were modeled using the additional parameters given for the ground surface (Table 2). The effects of vegetation are not considered in the heat storage estimation. Since the fraction of vegetation is very low, this should not have a large impact on the results.

The urban surface flux scheme, town energy balance (TEB), as described by Masson (2000), Masson et al. (2002), and Lemonsu et al. (2004) combined with a general land surface scheme (ISBA, Noilhan and Planton 1989) was used to estimate the surface to atmosphere exchange and heat storage fluxes. The parameters given in Table 2 were specified as inputs for the TEB model. Although four layers were used for each element (road, wall, roof), the depth-averaged properties were maintained. Bare soil was incorporated in the road surface fraction, so the ISBA scheme was used only for the vegetated surface (10%). This limits the overall sensitivity to ISBA input parameters. The vegetation was specified as tree cover with a leaf area index of 3 and an albedo of 0.15. The model was forced by the meteorological fields measured at DMN.

In addition to providing information about the dynamics of turbulent energy exchange between the sur-

face and atmosphere, the local-scale measurements of the energy balance allow for a comparison between the modeled heat storage flux and the residual computed from the local-scale flux observations, $\Delta Q_S = Q^* - Q_H - Q_E$. Although the residual incorporates unmeasured energy exchange components such as anthropogenic heat, these are believed to be small relative to the other components.

4. Results and discussion

a. Building-scale measurements and heat storage estimates

The structures examined differed primarily in terms of sky-view factors and materials for construction. PERI and CBD were measured concurrently (03/37–42), so only these two sites are compared directly. The downtown structure (CBD) was located on the roof of the hotel and had a concrete roof in contrast to the corrugated steel roof of PERI. Although the roof at PERI heats up more rapidly and to a higher degree due to the thin material, there is little storage and cooling is just as rapid (Fig. 6). The means of the four wall orientations (wall) temperatures are very similar until late afternoon when CBD continues to increase due to greater radiation loading on the west-facing wall. That the walls have very similar thermal response is expected given their estimated thermal properties (Table 2). The

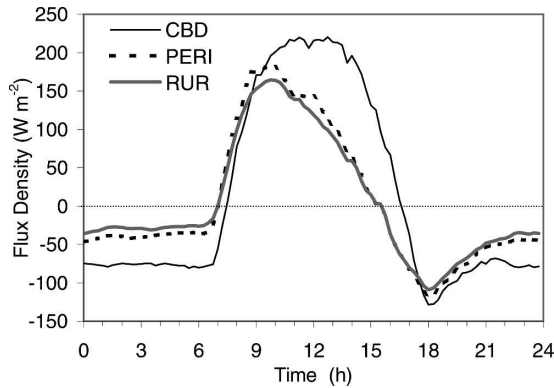


FIG. 7. Mean diurnal heat storage calculated from building scale observed temperatures (2003/38–40) and modeled soil temperature (RUR).

wall temperature measurements made later at RES are likewise very similar in the mean diurnal pattern and values to PERI. The room air temperature at CBD heats up quite rapidly to uncomfortable levels ($>35^{\circ}\text{C}$) during the daytime, but less so at PERI despite the greater roof temperature. The room at CBD was poorly ventilated and its floor was heated from below; the building's inside air temperature measured on the top floor did not drop below 30°C over the diurnal cycle. At night the PERI room air temperature also cools slowly, likewise attributed to poor ventilation but also may be due in part to the room being occupied.

The low thermal mass of the sheet metal roof, commonly used in residential areas, reduces heat storage relative to the predominantly concrete roofs in the urban center. However, the mean diurnal wall temperatures in both areas are about the same. Although the walls in both areas have similar thermal responses, particularly at night, the storage in walls will be much greater in the CBD case. Recent research has shown that much of the nighttime heat release in urban areas comes from the walls forming the urban canyon (Christen and Vogt 2004; Lemonsu et al. 2004; Offerle et al. 2005). This generally keeps the urban surface layer neutral or slightly unstable at night and contributes to the UHI effect. In the residential areas, owing to the low height and density of buildings, walls do not make up a large fraction of the thermal mass in the area. However, in the CBD the overall thermal mass of the walls is much greater and the reductions in sky-view factor are too small to sufficiently reduce the radiation loading to compensate. Figure 7 shows the patterns of local-scale heat storage modeled based on the observed surface temperatures for the different land covers (Table 2). Figure 7 highlights the differences between the different land uses. The modeled RUR is the heat storage

flux that might be expected for undeveloped areas largely devoid of vegetation, characteristic of the area surrounding Ouagadougou. It peaks rapidly, due to the low thermal conductivity such that at 0.2 m depth there is almost no diurnal variation in soil temperature. This also results in a rapid release of heat from storage in the late afternoon when, because of the high albedo, net longwave radiative losses exceed gains from net shortwave. In contrast, the heat storage flux from CBD lags the bare soil and continues to store heat for a longer portion of the day. Despite the more regulated average surface temperature, peak storage exceeds that of the rural surface. The periurban surface closely resembles that of the bare soil because the changes to thermal mass and the surface albedo are not so great. The CBD surface continues to release large amounts of heat throughout the night. This additional energy relative to the rural surface creates the nocturnal UHI effect.

The urban canopy layer heat island is not expected to be perfectly correlated with surface temperatures, but the patterns are quite similar. Figure 8 shows the mean horizontal surface temperature (based on surface cover fractions in Table 1) for the CBD and PERI site. The surface temperature difference is well correlated to differences in urban canopy layer air temperatures, although influenced by other factors such as wind speed and turbulence and the overall stability (e.g., diurnal differences in mixing height). Satellite-based remote sensing, which takes a nadir view of the surface and thus sees primarily horizontal surfaces (Voogt and Oke 2003), often records daytime cool islands in urban areas and nighttime heat islands, similar to Fig. 8. Although a daytime canopy layer cooling effect is not observed here, the CBD air temperature was measured at roof level (the top of the canopy layer). Another measurement site within the CBD at 2-m height recorded day-

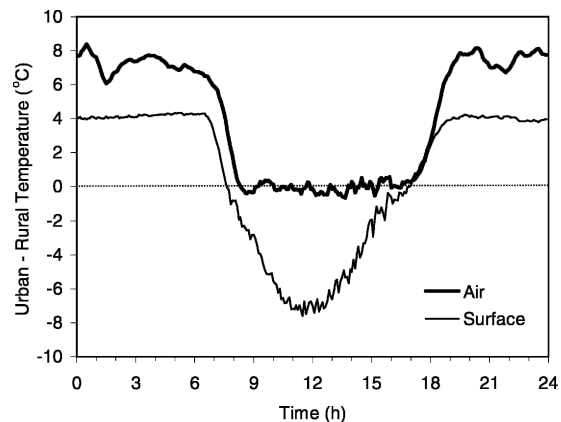


FIG. 8. Mean difference between urban (CBD) and rural (PERI) sites for air and horizontal surface (roofs, roads, soil) temperature (2003/37–42).

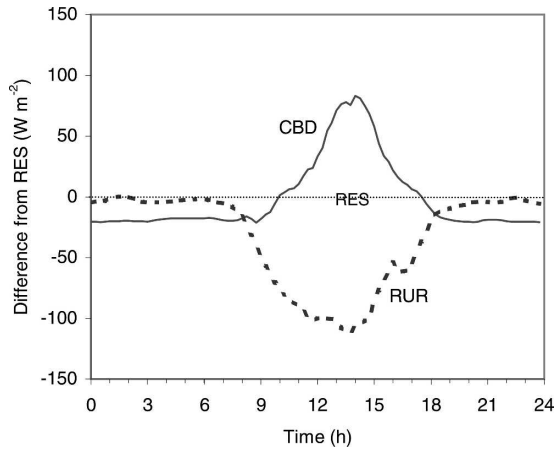


FIG. 9. Differences in net all-wave radiation from the residential site (RES) for different land uses (CBD mean for 5 days, RUR over 1 day).

time cooling of up to 2°C during the time of the measurements. That the air temperature pattern lags the surface temperature is expected since the air temperature must be coupled to the surface temperature via sensible heat fluxes.

b. Net radiation and remotely sensed surface characteristics

In addition to the differences in thermal characteristics, there are also differences in radiative characteris-

tics between the urban, residential, and periurban or rural areas. Although geometry and the amount of irrigated vegetation play a role, these factors may not be so important here. In Ouagadougou, as noted earlier, building heights are too low and too widely spaced to significantly reduce radiation loading on buildings or streets. In contrast to the periurban areas, many downtown streets are asphalt and have lower albedos than the unpaved, compacted soil. Irrigated vegetation is largely confined to areas near the reservoir (Fig. 1) and some wealthier neighborhoods. The CBD measurement location has nearly as little active vegetation as the rural areas. A comparison of net all-wave radiation between the different areas shows that net radiation is much greater during the daytime over the urban surface. The high albedo and high surface temperatures of the rural surface leads to lower net radiation throughout the day when compared with the residential surface (Fig. 9). At night net radiation over the rural and residential surfaces are similar, as was the case with heat storage flux (Fig. 8). The remotely sensed data agree with the information provided by the building-scale temperature observations and the net radiation measurements.

An east–west transect of the estimated albedo (30-m grid) is depicted in Fig. 10. Albedo varies spatially with the highest values over the rural areas. Albedo is approximately 15% greater in sector 29 (0.24) than in the downtown area (0.21) and at least 15% lower than in

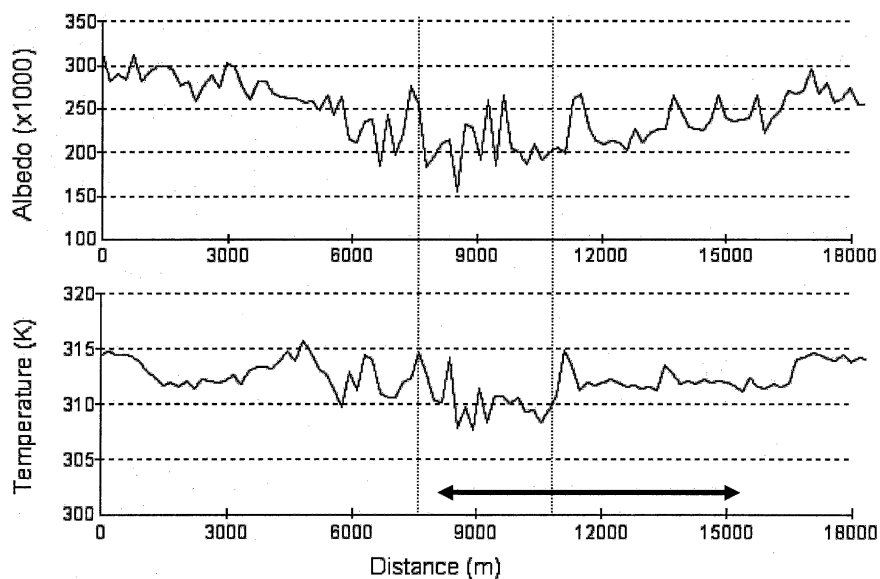


FIG. 10. Transects (100 equidistant points) of albedo and surface temperature across Ouagadougou from ASTER imagery (1030 LT 17 Jan 2001). The vertical lines mark the approximate extent of the downtown area on the transect; to the right is an extensive residential area, sector 29. The arrow marks the approximate extent of the transect shown on Fig. 1.

the outlying rural area (0.27–0.30). This in part explains why RES net radiation was $\sim 10\%$ lower than CBD and almost 20% greater than over the bare undisturbed soil (RUR). The bare soil surface temperature reached 61°C , more than 10°C greater than peak values measured on the same day at RES. This suggests that large outgoing longwave differences, on the order of 80 W m^{-2} , also contribute significantly to the daytime net radiation difference. The same transect for surface temperature (90-m spacing) is also shown in Fig. 10. Note that at the spatial resolution of the surface temperature image there is very little variation in residential or in the outlying areas although some large departures are apparent. Some of these are due to conspicuously large concrete structures, that is, an empty drainage ditch roughly marking the eastern edge of the city center. In the downtown there is slightly more variability due to shading and less homogenous land cover. The outlying areas are approximately 5°C warmer than the downtown, with the residential area roughly 2°C warmer than downtown. This pattern of temperatures is expected, given the earlier results, but the differences are smaller than suggested by Fig. 8. Because this was a January image, assuming the same atmospheric transmissivity, peak incoming solar radiation would be expected to be on the order of 100 W m^{-2} lower; thus these smaller temperature differences are not surprising. The difference seems to stem from the temperature of the rural surface. The spatial mean temperatures for downtown (37°C) and sector 29 (39°C) are close to the locally observed values for horizontal surfaces, which were both 39°C . However, the rural spatial mean (42°C) was less than the local observation (50°C).

The combined effect of the altered radiative and thermal properties on local climate is highlighted by the positive relation between albedo and surface temperature (Fig. 10). For surfaces with similar thermal characteristics, surface temperature should have an inverse relation with albedo; that is, the higher the albedo the lower the absorbed solar radiation and thus lower surface temperature. In the dry season, thermal characteristics are sufficiently different such that this is not the case. In the rainy season, the moisture content of the soil makes it darker and increases both thermal conductivity and heat capacity, which serve to increase absorbed and stored net radiation during the day. Verhoef et al. (1999) measured a change in albedo from October to January of 0.17 to 0.24 over a Sahelian savannah. Thus, in the rainy season, differences between the city and its rural surroundings in thermal and radiative characteristics are not as exaggerated. Although influenced by increased cloud cover and atmospheric moisture during the rainy season, the seasonality of the

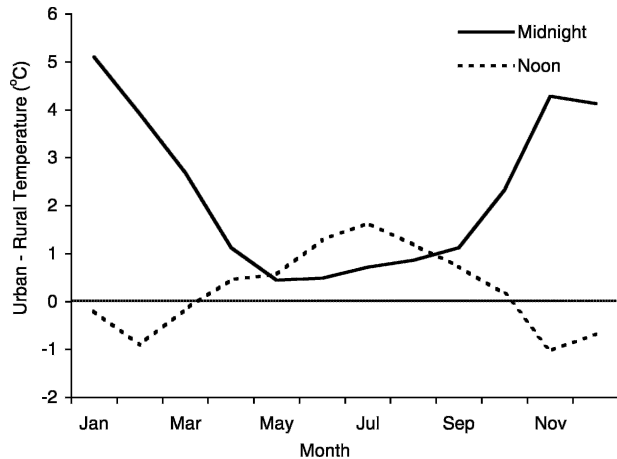


FIG. 11. Seasonality of urban (CBD) – rural temperature difference. Monthly mean temperature difference for midnight and noon for the period Feb 2002–Jan 2003.

urban – rural temperature difference reflects the seasonal changes in the rural surface characteristics (Fig. 11).

c. Local-scale measurements and modeling

The turbulent fluxes measured over the residential area provide a more complete picture of the energy balance dynamics. As can be expected at this time of year, the energy exchange with the atmosphere is dominated by Q_H with large changes in stored heat in the surface elements. Figure 12 shows the energy balance components for the RES area measured from the tower and the TEB–ISBA model results for the RES parameters. Both show similar patterns and magnitudes for the components although the modeled value has slightly greater storage, and lower Q^* in the afternoon owing to higher surface temperatures or lower turbulent exchange (Table 3). The modeled turbulent sensible heat fluxes also lag those of the observations.

Latent heat fluxes, although small, are not insignificant and could be greater than expected. The Q_E flux averaged 20 W m^{-2} over all measurements and the midday (10–14 h) Bowen ratio ($\beta = Q_H/Q_E$) had a mean of 3.7 (Table 3), ranging from 2–6 over the days measured. Tree cover (the only vegetation apparent) is sparse and estimated at around 10%, although most compounds had shade trees (Fig. 4). Studies over urban environments with similar low fractions of vegetation suggest that a β between 3 and 10 is typical, although these sites were in North American cities with considerably more impervious surface (Grimmond and Oke 2002). A comparison could be made with the Sahelian flux measurements, Sahelian Energy Balance Experi-

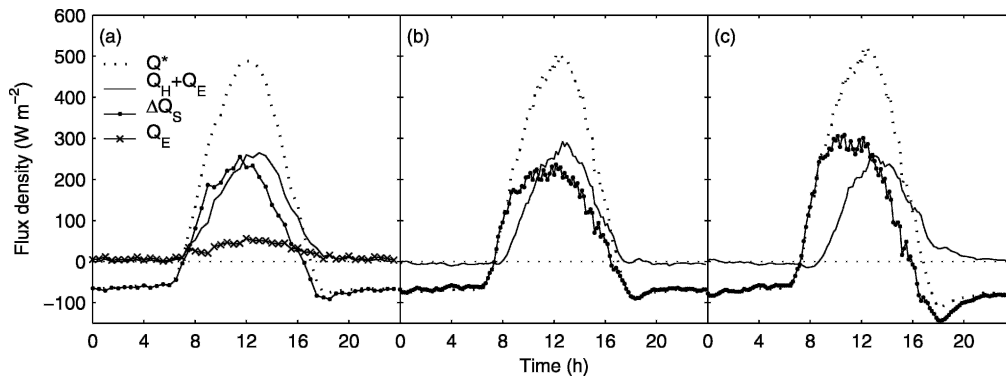


FIG. 12. Ensemble diurnal energy balance components for RES for the period 2003/39–51, excluding 48 because of incomplete data. (a) Measured components and ΔQ_S (residual; 30-min averages). (b) Components modeled with TEB-ISBA (10-min averages). (c) Same as (b) but for CBD parameters.

ment (SEBEX) and Hydrologic–Atmospheric Pilot Experiment in the Sahel (HAPEX-Sahel), (Goutorbe et al. 1997); however, no direct measurements of sensible and latent heat fluxes were made at this time of year. Based on an empirical formulation, Verhoef et al. (1999) estimated average dry season Q_E for a Sahelian savannah site to be around 10 W m^{-2} . Given that the vegetation here consists mainly of trees, a higher Q_E is not unreasonable. The higher Q_E also does not require water uptake from deeper soil layers. Data on household water consumption for Ouagadougou in February 2002 (ONEA 2003, personal communication) indicate that domestic water usage could account for a Q_E of up to 25 W m^{-2} . Other sources, such as combustion from outdoor wood-fueled cooking stoves and vehicle exhaust (mopeds and cars), are thought to be relatively small and the diurnal pattern in Q_E does not show a strong signal from these sources.

The diurnal Q_H remained slightly positive for about an hour after sunset. Primarily neutral to stable conditions were observed at night with very low wind speeds. Thus, although the magnitude of the heat storage flux has increased, the dynamics of the exchange in this residential area does not appear drastically different than

could be expected over the dry rural areas. In contrast, the model results for the CBD (Fig. 12c) show much greater daytime heat storage and more delayed turbulent heat flux response. The model also predicts continued positive sensible heat fluxes several hours into the night.

While the objective here was not to evaluate the performance of TEB, such evaluations are necessary to determine how well the urban energy balance is represented before possible impacts of urban growth on local climate can be considered. Aside from the above noted differences in the timing fluxes, the model is in good agreement with the flux observations at RES. The unsystematic root-mean-square differences (URMSD) from the diurnal ensembled observations was less than 15 W m^{-2} for Q^* and the residual determined ΔQ_S . While latent and sensible heat fluxes were not individually compared, their sum was also in good agreement ($\text{URMSD} < 15 \text{ W m}^{-2}$).

5. Conclusions

Although urban sprawl and unplanned periurban development in rapidly expanding tropical cities may create numerous social problems, their impacts on local climate may be less drastic than planned developments within the city. Periurban and most existing residential areas in Ouagadougou have characteristics that are more similar to the current rural surroundings than does the downtown. Grading and compaction of the surface for roads and increasing density of compound houses have a measurable impact in terms of net radiation and heat storage, but less than those of a paved or densely built surface. The difference in net radiative exchange between the residential and CBD areas is an important factor for the local climate. Net radiation is greater downtown during the dry season because, in

TABLE 3. Summary of mean measured and modeled energy balance components at RES in W m^{-2} where β (unitless) is the Bowen ratio (Q_H/Q_E) calculated from the means in the table. Data are for days 2003/39–51 excluding 48 owing to incomplete data.

	Hours	Q^*	Q_H	Q_E	ΔQ_S	β
Observed	All	88.9	50.6	20.5	17.8	2.5
	1100–1400	464.3	192.2	51.9	220.2	3.7
TEB-ISBA	All	79.7	59.0	20.7		
	1100–1400	459.4	252.8	206.6		

addition to the higher albedo, the dry bare soil and the metal roofing, predominant in residential and periurban areas, heat up more quickly than the CBD surface, thus offsetting the typical differences in outgoing long-wave radiation. Another important factor is the difference in heat storage fluxes due to geometry and material properties. Although sheet metal roofing may not give the ideal indoor environment, it will have a smaller impact on the outdoor environment. The more massive CBD stores much more heat over the day. If increased urbanization leads to increased reliance on nonlocal materials, more paving and increasing height and density of buildings will affect the surface energy balance by decreasing albedo and increasing heat storage, leading to higher nighttime urban temperatures. The impacts of increased urbanization were not assessed for the rainy season.

The measurements described here provide a valuable resource to calibrate and evaluate the performance of models that can be used to evaluate the impacts of potential changes in urban surface characteristics. The model used here, TEB (Masson 2000), was shown to compare well with measured fluxes over a residential area, the most extensive land use in Ouagadougou. This suggests that TEB is applicable for use in climate and mesoscale models to address larger scales (urban, meso, etc.) in this region. These results encourage us that such methods can be applied to examine land cover change impacts on urban and larger-scale climate.

Acknowledgments. We thank the following organizations and persons for providing access to sites and data: Direction de la Météorologie Nationale du Burkina Faso, Frédéric Ouattara, Director, Oumarou Ouedraogo, Technical Supervisor; Telecel Burkina, Direction Générale and Harouna Tinta. Valery Masson provided the TEB model code. This work was supported by grants from the National Science Foundation (BCS-0095284, SG; 0221105, SG+BO), Indiana University (PCIP, SG), and the Swedish International Development Cooperation Agency (PJ+IE).

REFERENCES

- Ahmed, K. S., 2003: Comfort in urban spaces: Defining the boundaries of outdoor thermal comfort for the tropical urban environments. *Energ. Build.*, **35**, 103–110.
- Ben Mohamed, A., N. Van Duivenboden, and S. Abdoussallam, 2002: Impact of climate change on agricultural production in the Sahel—Part 1. Methodological approach and case study for millet in Niger. *Climate Change*, **54**, 327–348.
- Binns, J. A., R. A. Maconachie, and A. I. Tanko, 2003: Water, land and health in urban and periurban food production: The case of Kano, Nigeria. *Land Degrad. Develop.*, **14**, 431–444.
- Christen, A., and R. Vogt, 2004: Energy and radiation balance of a central European city. *Int. J. Climatol.*, **24**, 1395–1421.
- Chrysoulakis, N., 2003: Estimation of the all-wave urban surface radiation balance by use of ASTER multispectral imagery and in situ spatial data. *J. Geophys. Res.*, **108**, 4582, doi:10.1029/2003JD003396.
- Eklundh, L., and L. Olsson, 2003: Vegetation index trends for the African Sahel 1982–1999. *Geophys. Res. Lett.*, **30**, 2003, doi:10.1029/2002GL016772.
- Gerstl, S., 2001: The economic costs and impact of home gardening in Ouagadougou, Burkina Faso. Ph.D. thesis, University of Basel, 426 pp.
- Goutorbe, J. P., and Coauthors, 1997: An overview of HAPEX-Sahel: A study in climate and desertification. *J. Hydrol.*, **189**, 4–17.
- Grimmond, C. S. B., and T. R. Oke, 2002: Turbulent heat fluxes in urban areas: Observations and a local-scale urban meteorological parameterization scheme (LUMPS). *J. Appl. Meteor.*, **41**, 792–810.
- Helbig, A., J. Baumüller, and M. J. Kerschgens, 1999: *Statklima und Luftreinhaltung*. Springer-Verlag, 467 pp.
- Jauregui, E., L. Godinez, and F. Cruz, 1992: Aspects of heat-island development in Guadalajara, Mexico. *Atmos. Environ.*, **26B**, 391–396.
- Landsberg, H. E., 1981: *The Urban Climate*. Academic Press, 275 pp.
- Lemonsu, A., C. S. B. Grimmond, and V. Masson, 2004: Modeling the surface energy balance of an old Mediterranean city core. *J. Appl. Meteor.*, **43**, 312–327.
- Liang, S., 2000: Narrowband to broadband conversions of land surface albedo. I. Algorithms. *Remote Sens. Environ.*, **76**, 213–238.
- Masson, V., 2000: A physically-based scheme for the urban energy balance in atmospheric models. *Bound.-Layer Meteor.*, **94**, 357–397.
- , C. S. B. Grimmond, and T. R. Oke, 2002: Evaluation of the town energy balance (TEB) scheme with direct measurements from dry districts in two cities. *J. Appl. Meteor.*, **41**, 1011–1026.
- Nasrallah, H. A., J. Brazel, and R. C. Balling, 1990: Analysis of the Kuwait City urban heat island. *Int. J. Climatol.*, **10**, 401–405.
- Nicholson, S. E., and J. P. Grist, 2001: A conceptual model for understanding rainfall variability in the West African Sahel on interannual and interdecadal timescales. *Int. J. Climatol.*, **21**, 1733–1757.
- Noilhan, J., and S. Planton, 1989: A simple parameterization of land surface processes for meteorological models. *Mon. Wea. Rev.*, **117**, 536–549.
- Offerle, B., 2003: The energy balance of an urban area: Examining temporal and spatial variability through measurements, remote sensing and modeling. Ph.D. thesis, Indiana University, 220 pp.
- , C. S. B. Grimmond, K. Fortuniak, K. Klyzik, and T. R. Oke, 2005: Temporal variations in heat fluxes over a central European city centre. *Theor. Appl. Climatol.*, in press.
- Oke, T. R., 1987: *Boundary Layer Climates*. Routledge, 435 pp.
- UNPOP (Population Division of the Department of Economic and Social Affairs of the United Nations Secretariat), 2002: World Urbanization Prospects: The 2001 Revision. [Available online at <http://www.un.org/esa/population/publications/wup2001/wup2001dh.pdf>.]

- Van Deursen, W., A. Bagre, S. de Jong, and P. van Teeffellen, 1999: Monitoring trends in urban growth: Ouagadougou, Burkina Faso. Netherlands Remote Sensing Board, BCRS-project 3.1/DE-11, 55 pp.
- van Dijk, A., W. Kohsiek, and H. A. R. de Bruin, 2003: Oxygen sensitivity of krypton and Lyman- α hygrometers. *J. Atmos. Oceanic Technol.*, **20**, 143–151.
- Verhoef, A., S. J. Allen, and C. R. Lloyd, 1999: Seasonal variation of surface energy balance over two Sahelian surfaces. *Int. J. Climatol.*, **19**, 1267–1277.
- Voogt, J. A., and T. R. Oke, 2003: Thermal remote sensing of urban climates. *Remote Sens. Environ.*, **86**, 370–384.
- Vose, R. S., R. L. Schmoyer, P. M. Steurer, T. C. Peterson, R. Heim, T. R. Karl, and J. K. Eischeid, 1998: The global historical climatology network: Long-term monthly temperature, precipitation, sea level pressure, and station pressure data. ORNL/CDIAC-53, CDIAC NDP-041, Carbon Dioxide Information Analysis Center, Oak Ridge National Laboratory, Oak Ridge, TN. [Available online at <http://www.daac.ornl.gov>.]